

DAMEL: Dual-Axis Multi-Expert Learning for Class-Imbalanced Learning

Hyuck Lee^{a,1}, Taemin Park^{b,1}, Heeyoung Kim^b

^a*AI Research, Krafton, Teheran-ro 231, Centerfield EAST, Gangnam-gu, Seoul, 06142, Republic of Korea*

^b*Department of Industrial and Systems Engineering, Korea Advanced Institute of Science and Technology (KAIST), 291 Daehak-ro, Yuseong-gu, Daejeon, 34141, Republic of Korea*

Abstract

Various algorithms have been proposed to address the challenges posed by class-imbalanced learning from real-world data with long-tailed distributions. While these algorithms reduce prediction bias through rebalancing techniques, they often introduce increased prediction variance as a trade-off. Several multi-expert learning algorithms aim to address this variance but involve complex procedures. We propose a new multi-expert learning algorithm, called the dual-axis multi-expert learning (DAMEL), which reduces both bias and variance of predictions by using multiple experts along both representation and time axes. Along the representation axis, DAMEL concatenates the representations of multiple experts and trains an auxiliary balanced classifier simultaneously with the concatenated representations. Along the time axis, DAMEL aggregates network weights across training epochs, employing these aggregated weights during testing. Experimental results demonstrate that DAMEL reduces both bias and variance of predictions, highlighting its effectiveness in class-imbalanced learning.

Keywords: Long-tailed learning, Multi-expert learning, Exponential moving average of weights.

Email addresses: dlgur0921@kaist.ac.kr (Hyuck Lee), ptm1001@kaist.ac.kr (Taemin Park), heeyoungkim@kaist.ac.kr (Heeyoung Kim)

¹Equal contribution

1. Introduction

Deep neural networks (DNNs) have demonstrated remarkable performance across a wide range of tasks, owing to their ability to capture complex patterns and perform large-scale computations efficiently [33, 35, 73]. However, many real-world datasets exhibit class imbalance, which poses a significant challenge for training classification models, often leading to a bias toward majority classes [7, 9, 15, 39, 53, 72]. To address this issue, a variety of class-imbalanced learning (CIL) methods have been proposed. Existing CIL techniques include rebalancing the class distribution with resampling [2, 6, 21, 29, 42, 54] and reweighting [25, 40, 50, 66, 77], decoupled learning [31, 55], and data augmentation [8, 34, 75]. These techniques have successfully improved the classification accuracy.

However, it was recently reported that these CIL techniques tend to increase the variance of the predictions at the cost of reducing the squared bias of the predictions [64]. To reduce the variance of the predictions, ensemble strategies, which involve training multiple experts, have been proposed [4, 64, 69, 78]. By reducing the variance of the predictions, multi-expert learning algorithms achieved higher classification accuracy compared to other CIL techniques. However, they require multi-stage learning with knowledge distillation or division of the training data into multiple groups for training each expert, making implementation of the algorithms difficult.

In this paper, we propose a new multi-expert learning algorithm for CIL, called the dual-axis multi-expert learning (DAMEL), that uses multiple experts along the representation and time axes in a conceptually simple manner. Specifically, DAMEL can reduce both the squared bias and the variance of the predictions compared to existing multi-expert learning algorithms owing to the following major changes: 1) whereas other multi-expert learning algorithms aggregate the predictions of multiple experts, DAMEL aggregates the representations of multiple experts and trains an auxiliary classifier with a class-balanced loss using the aggregated representations; 2) DAMEL also aggregates the weights of the neural network at the end of each epoch, which can be understood as an ensemble along the time axis. DAMEL can be trained in one stage without complex processes such as knowledge distillation or complicated splits of training data.

Specifically, the multiple experts of DAMEL share a deep CNN up to the last residual block as a backbone to reduce computational cost, similar to previous multi-expert learning algorithm [4, 64]. Then, DAMEL has indi-

Table 1: Summary of recent multi-expert learning algorithms

Algorithm	Data split	One-stage/Multi-stage	Ensemble of experts	Time axis ensemble
BBN [78]	O	One-stage learning	Classifier	X
LFME [69]	O	Multi-stage learning	Classifier	X
RIDE [64]	X	Multi-stage learning	Classifier	X
ACE [4]	O	One-stage learning	Classifier	X
TLC [44]	X	One-stage learning	Classifier	X
ResLT [12]	X	One-stage learning	Classifier	X
DAMEL (Ours)	X	One-stage learning	Representations	O

vidual last residual blocks with classification layers, each of which is trained independently using the cross-entropy loss. It is known that each expert learns different representations even if it is trained with the same loss, because different initializations of network weights lead to different modes in the optimization process [20, 38, 52]. To use the various representations that multiple experts learn from various modes, we concatenate the last representation layers of the multiple experts and train an auxiliary classifier with a class-balanced loss using the concatenated representations. Training the auxiliary classifier with the aggregated representations in this way reduces both the squared bias and the variance of the predictions because the auxiliary classifier can use various representations from all experts. Contrary to a recent trend to decouple the learning of representations and the classifier, we train the auxiliary classifier and multiple experts end-to-end, so that the classifier can be compatibly trained with the representations [41, 63]. In Section 3, we explain why aggregating representations is better than aggregating the predictions of multiple experts.

In addition to aggregating representations, we aggregate the network weights at the end of each epoch to reduce the variability in the weights and, consequently, the variance of the predictions. We aggregate the weights using the exponential moving average (EMA) at the end of each epoch, so that we can prioritize the weights of the network trained with more epochs. We aggregate the weights at the end of each epoch, not at each iteration, because it is known that an ensemble of predictions becomes more effective as the correlation among the predictions is lower [48]. The EMA weights are

automatically updated by the weights of the trained network. We use the EMA weights to predict the class labels of new data points in the test phase. The aggregation of the weights using the EMA lowers the variance of the predictions because of the effect of the ensemble along an additional axis. Using the EMA weights also reduces the squared bias of the predictions because the aggregated weights stably approach the local optima [27] in the test error surface with a constant learning rate. The main difference between DAMEL and other multi-expert learning algorithms are summarized in Section 1.

Our experimental results on CIFAR-10-LT, CIFAR-100-LT [14], ImageNet-LT [47], and iNaturalist2018 [62] under various scenarios demonstrate that DAMEL achieves highest accuracy in CIL experiments. Through an extensive experimental analysis, we verify that using aggregated representations of multiple experts as well as the aggregated weights of the network reduces both the squared bias and the variance of the predictions compared to existing multi-expert learning algorithms. We also investigate the contribution of each component of DAMEL through an ablation study. The main contributions of this paper are summarized as follows:

- We introduce a representation-axis ensemble that aggregates expert representations by concatenation, rather than averaging representations or aggregating predictions, allowing the auxiliary classifier to exploit complementary features learned by different experts.
- We show that representation concatenation in DAMEL is not merely an increase in feature dimensionality, but a mechanism for preserving expert-specific representation diversity and jointly utilizing discriminative cues captured by multiple experts.
- We introduce a time-axis ensemble based on epoch-level EMA weight aggregation, which differs from conventional iteration-level EMA and SWA by treating temporally aggregated weights as an additional ensemble axis for reducing prediction variance.
- We design an auxiliary balanced classifier trained on concatenated expert representations with a class-balanced loss, enabling the classifier to reduce prediction bias toward majority classes while leveraging diverse expert features in one-stage learning.
- We demonstrate through extensive experiments and ablation studies that the proposed representation-axis and time-axis ensembles jointly

reduce both squared bias and prediction variance, leading to improved performance on long-tailed benchmarks.

2. Related Work

Class-Imbalanced Learning: Traditional approaches to address class imbalance include resampling and reweighting techniques. Resampling techniques [2, 6, 21, 29] balance the class distribution by adjusting the amount of data in each class, and reweighting techniques [25, 50, 66, 77] assign higher weights to the minority class during training. While these techniques are simple to implement, they often suffer from overfitting, information loss, and unstable training [1, 5]. To address these issues, Cui [14] proposed a reweighted loss based on an effective number of data points, and Jamal [28] and Ren [56] proposed meta-learning based reweighting. Cao [5] and Ren [55] minimized a generalization error bound with a new loss function. Kim [34] and Yin [71] transferred knowledge acquired from the majority class data to the minority classes. Kang [31] decoupled learning of representations and training of the classifier. Menon [49] proposed a logit-adjusted loss, which is Fisher consistent for the balanced error. Wei [67] and Jada [74] supplemented the minority class data using out-of-distribution data and pure noise images, respectively. Recently, studies of contrastive learning [13, 30, 45, 63], class-balanced distillation [26, 46], and multi-expert learning [4, 44, 64, 69, 78] have received attention. We focus on multi-expert learning.

Multi-Expert Learning: Various multi-expert learning algorithms have been proposed to reduce the variance of predictions. BBN [78] trains an over-balanced classifier and an imbalanced classifier together, and aggregates the predictions of the two classifiers. LFME [69] assigns an expert to each non-overlapping class group and aggregates the predictions of multiple experts through knowledge distillation. RIDE [64] uses an individual expert classification loss and distribution-aware diversity loss to diversify multiple experts. ACE [4] distributes diverse but overlapping class splits for each expert, so that multiple experts can be supportive and complementary. TLC [44] estimates uncertainty of each expert, and assigns high importance to trustworthy experts in the test phase. ResLT [12] employs a residual fusion mechanism, utilizing a main branch for all classes and two residual branches to enhance the medium and tail classes. Whereas these algorithms aggregate the predictions of multiple experts, we aggregate the representations. In addition, we

ensemble the weights of the neural network along the time axis using EMA weights in the test phase.

Exponential Moving Average of Weights: Recently, EMA weights have been used in various deep learning algorithms. For example, Tarvainen and Valpola [61] used EMA weights for the consistency regularization of semi-supervised learning algorithms. He [22] used EMA weights to build a consistent memory module for contrastive learning. Tan [59]; Howard [24]; Tan and Le [60] used EMA weights to stabilize the optimization process. Fan [19] used EMA weights to build a momentum encoder in imbalanced semi-supervised learning. Unlike these studies, we interpret the EMA weights as ensembles along the time axis and analyze averaging network weights along time axis in detail in terms of squared bias and variance. In addition, whereas other studies update the EMA weights for each iteration, we update them for each epoch to increase the diversity of the weights to be aggregated.

Stochastic Weight Averaging (SWA): Izmailov [27] proposed SWA, which simply averages the weights of a network along the time axis to stabilize the optimization process and make the weights closer to the local optima in the test loss surface. SWA is similar to EMA of weights in that it averages the weights along the time axis, but SWA cannot prioritize the weights of the network trained with more epochs. In Section 4.8, using the EMA of weights is shown to be more effective than SWA.

3. Methodology

3.1. Problem Setting

Suppose that we have a training set $\mathcal{D} = \{(x_n, y_n) : n \in (1, \dots, N)\}$, where $x_n \in \mathbb{R}^d$ is the n th data point and $y_n \in \{1, \dots, L\}$ is the corresponding label. We denote the number of data points belonging to class l as N_l , i.e., $\sum_{l=1}^L N_l = N$, and without loss of generality, we assume that the L classes are sorted according to cardinality in descending order, i.e., $N_1 \geq N_2 \geq \dots \geq N_L$. We denote the ratio of the class imbalance as $\gamma = \frac{N_1}{N_L}$ and $\gamma \gg 1$ under class-imbalanced scenarios. From \mathcal{D} , we generate minibatches $\mathcal{MB} = \{(x_b, y_b) : b \in (1, \dots, B)\} \subset \mathcal{D}$ for each iteration of training, where B is the minibatch size. Using these minibatches for training, we aim to learn a classification algorithm $f : \mathbb{R}^d \rightarrow \{1, \dots, L\}$ that performs effectively on a class-balanced test set $\mathcal{D}_{test} = \{(x_m, y_m) : m \in (1, \dots, M)\}$.

It is well known that there is a trade-off between the squared bias and the variance of the predictions, but we can reduce the variance without increasing

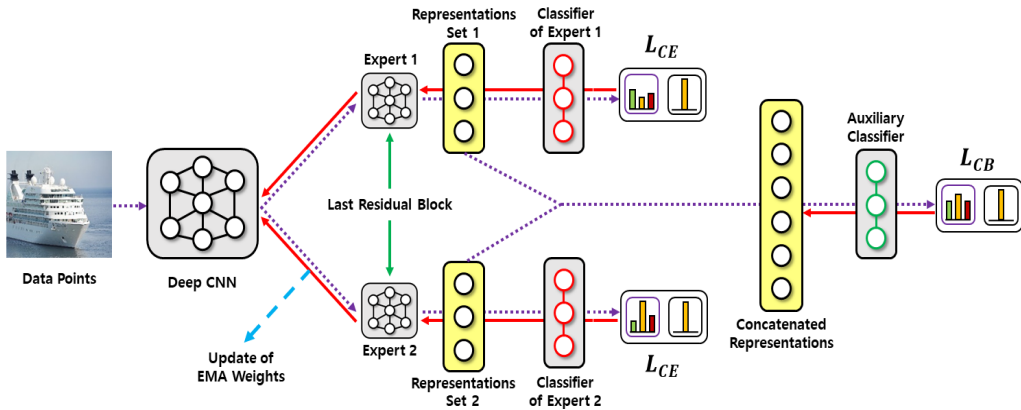


Figure 1: Overall structure of DAMEL (two experts). Purple lines indicate forward propagation, red lines indicate gradients, and the blue line indicates the updating of EMA weights at the end of each epoch. An auxiliary classifier with EMA weights is used in the test phase.

the squared bias by using an ensemble strategy. Specifically, if we assume that the class-imbalanced training set \mathcal{D} is randomly drawn from the underlying true distribution, we can treat \mathcal{D} as a random variable. Then, the expectation of the squared prediction error $\mathbb{E}_{\mathcal{D}}[\sum_{m=1}^M (y_m - f_{\mathcal{D}}(x_m))^2]$ can be decomposed into the sum of the squared bias $\sum_{m=1}^M (y_m - \mathbb{E}_{\mathcal{D}}[f_{\mathcal{D}}(x_m)])^2$, variance $\mathbb{E}_{\mathcal{D}}[\sum_{m=1}^M (f_{\mathcal{D}}(x_m) - \mathbb{E}_{\mathcal{D}}[f_{\mathcal{D}}(x_m)])^2]$, and irreducible error of the predictions [36], where $f_{\mathcal{D}}$ is a classification algorithm trained with randomly drawn training set \mathcal{D} . The ensemble of multiple experts can reduce more variance as the correlation between the predictions of multiple experts decreases and the number of experts increases. To effectively ensemble multiple experts without a significant increase in computational complexity, we aggregate the representations of multiple experts and aggregate the weights at the end of each epoch. As described in Section 3.3 and Section 3.5, our ensemble strategy also reduces the squared bias of the predictions.

3.2. Learning Various Representations

By individually training multiple experts, we ensure that DAMEL learns various representations. Specifically, DAMEL uses K experts that share a backbone $g(\cdot)$ and have individual last residual blocks $h_k(\cdot)$ with single-layer classifiers that have weights w_k , $k \in \{1, \dots, K\}$. We denote the output of the k th expert before its classification layer as $h_k \circ g(x_b) = z_k$, where z_k is the set of the k th representations. Then, the prediction of the k th

expert $p_k(y|x_b)$ can be calculated as $\text{softmax}(\alpha\bar{w}_k^T\bar{z}_k)$, where \bar{w}_k^T and \bar{z}_k denote the L2 normalized versions of w_k^T and z_k , respectively, and α is a scale hyperparameter. We individually train each expert with the cross-entropy loss as follows:

$$L_{CE}^k = \sum_{b=1}^B \text{CELoss}(y_b, p_k(y|x_b)), \quad (1)$$

where CELoss denotes the cross-entropy loss. Even though each expert is trained with the same loss, it learns different representations because the neural network with different initializations finds a different mode in the optimization process [38, 52]. In terms of exploring multiple modes, the training of multiple experts can be viewed similarly to Bayesian neural networks [3, 68], but it is more effective because a deep ensemble strategy can explore various modes than Bayesian neural networks [20]. In Section 4.3, we verify that each expert learns different representations.

3.3. Training the Auxiliary Classifier

DAMEL reduces both the squared bias and the variance of predictions using various representations learned by multiple experts. Specifically, multiple sets of representations are first concatenated and then an auxiliary classifier is trained using the concatenated representations with a class-balanced loss. Here, we aggregate the representations of multiple experts $\bar{z}_k, k = 1, \dots, K$, by concatenation, not averaging, to preserve their diversity. Using the concatenated representations, the prediction from the auxiliary classifier $p(y|x_b)$ can be calculated as $\text{softmax}(\alpha\bar{w}^T\bar{z})$, where \bar{w} denotes the L2 normalized weights of the auxiliary classifier and \bar{z} denotes the concatenated representations $[\bar{z}_1, \dots, \bar{z}_K]$. We train the auxiliary classifier with a class-balanced loss as follows:

$$L_{CB} = \sum_{b=1}^B \text{CBLoss}(y_b, p(y|x_b)), \quad (2)$$

where CBLoss reweights the cross-entropy loss for each class by a factor that is inversely proportional to the quantity of data for the class. Recently, it has been found that training networks with class-balanced losses results in learning representations of lower quality than training with cross-entropy loss [31]. Considering this finding, we train only the auxiliary classifier with gradients backpropagated from CBLoss and detach the gradients backpropagated to the concatenated representations.

Unlike existing multi-expert learning algorithms, DAMEL aggregates representations, not predictions, of multiple experts, and produces predictions using the auxiliary classifier. This allows the auxiliary classifier to receive the information from the representations of all the experts. Using such richer information, the auxiliary classifier can produce more accurate predictions (i.e., the auxiliary classifier can lower the squared bias of the predictions). By contrast, if we train multiple auxiliary classifiers and aggregate their predictions as in the existing algorithms, each auxiliary classifier will produce predictions using the representations of a single expert only. In Section 4.3, we verify that aggregating the representations of multiple experts results in better performance than aggregating predictions by reducing the squared bias as well as the variance of the predictions.

3.4. End-to-End Training of DAMEL

Unlike the recent trend of CIL to decouple the learning of representations and class-balanced classifiers [31], we train the auxiliary classifier and multiple experts of DAMEL end-to-end with the total loss L_{total} as follows:

$$L_{total} = L_{CB} + \sum_{k=1}^K L_{CE}^k. \quad (3)$$

End-to-end training of DAMEL encourages the auxiliary classifier to be trained compatibly with the concatenated representations [41, 63]. In Section 4.8, we show that end-to-end training of DAMEL produces better performance than the decoupled training of multiple experts and the auxiliary classifier of DAMEL.

In the test phase, we use the predictions of the auxiliary classifier only, excluding the predictions of multiple experts, because they are not trained with the class-balanced loss. Overall structure of DAMEL is presented in Section 1.

3.5. EMA Weights of Network

To enjoy the ensemble effect of using multiple experts along the time axis, we also aggregate the network weights at the end of each epoch so that we can reduce the variability of the network weights and, consequently, the variance of the predictions. Let θ denote the whole weights of the neural network trained with the total loss in Equation (3). We introduce the EMA

weights θ_{EMA} obtained by aggregating θ at the end of each epoch using the EMA as follows:

$$\theta_{EMA}^t = (1 - \beta) \times \theta_{EMA}^{t-1} + \beta \times \theta, \quad (4)$$

where θ_{EMA}^t denotes the EMA weights at the t th epoch and β is an EMA update hyperparameter. The weights of the network θ are independently trained with aggregated weights θ_{EMA} , and DAMEL only uses θ_{EMA} in the test phase. As shown in Equation (4), θ_{EMA} is not trained by backpropagated gradients from losses, but it is automatically updated using θ . Therefore, the increased complexity of the algorithm owing to the use of the EMA weights is not significant. The only additional task is to compute the running mean and standard deviation of each layer of the network with θ_{EMA} , which are required for batch normalization of the test set. These statistics can be simply computed by propagating the training set forward before the test phase.

Using the ensemble along the additional axis of time, we can further lower the variance of the predictions compared to existing multi-expert learning algorithms. It is known that the variance of ensembled predictions decreases as the correlation among the component predictions decreases. Based on this, we update θ_{EMA} for each epoch, rather than for each iteration, to increase the diversity of the component weights of the ensemble.

In addition to reducing the variance of predictions, the use of EMA weights also reduces the squared bias of predictions because the aggregated weights stably approach wide local optima [27], which are approximately optimal even with small perturbations. This stable optimization process makes it possible to maintain a high learning rate, which leads to the convergence of the test loss to a low value, as we analyze in Appendix A. We present confusion matrices of the predictions on the test set of CIFAR-10 [37] in Appendix B to show that the use of EMA weights reduces the squared bias of predictions for minority classes.

The use of EMA weights can provide a universal framework for CIL or other tasks. We present the pseudocode for the training procedure of DAMEL in Section 1. The for-loops in the algorithm can be executed in parallel.

Algorithm 1 Training procedure of DAMEL

Input: $\mathcal{MB} = \{(x_b, y_b) : b \in (1, \dots, B)\} \subset \mathcal{D}$
Output: Weights of the network θ , θ_{EMA}
while training **do**
 for $b = 1$ to B **do**
 for $k = 1$ to K **do**
 $z_k = h_k \circ g(x_b)$
 $p_k(y|x_b) = \text{softmax}(\alpha \bar{w}_k^T \bar{z}_k)$
 Calculate $L_{CE+}^k = \text{CELoss}(y, p_k(y_b|x_b))$
 end for
 Concatenated representations $z = [z_1, \dots, z_k]$
 $p(y|x_b) = \text{softmax}(\alpha \bar{w}^T \bar{z})$
 Calculate $L_{CB+} = \text{CBLoss}(y, p(y_b|x_b))$
 end for
 Total loss $L_{total} = L_{CB} + \sum_{k=1}^K L_{CE}^k$
 $\Delta\theta \propto \nabla_{\theta} L_{total}$, $\theta \leftarrow \theta + \Delta\theta$
 if Epoch ends **then**
 $\theta_{EMA}^t = (1 - \beta) \times \theta_{EMA}^{t-1} + \beta \times \theta$
 end if
end while

4. Experiments

4.1. Experimental Setup

CIFAR-10-LT and **CIFAR-100-LT** [14] are artificially created long-tailed datasets from CIFAR-10 and CIFAR-100 [37], respectively, where the number of data points exponentially decreases from N_1 to N_L , i.e., $N_k = N_1 \times (N_L/N_1)^{\frac{k-1}{L-1}}$. The size of each image is 32×32 , and the images were augmented with random crop and horizontal flip. We conducted experiments on CIFAR-10-LT and CIFAR-100-LT [14] while changing the ratios of the class imbalance γ from 100 to 50. For the experiments on CIFAR-100-LT, we categorized the classes into three groups: Many (classes with more than 100 training data points), Medium (classes with 20–100 training data points), and Few (classes with less than 20 data points), following [47]. We measured group-wise accuracy and overall accuracy following baseline algorithms (e.g., BBN, LFME, ACE, RIDE, TLC). (Note that whereas metrics such as precision/recall/F-1/AUC are frequently reported in binary-class

class-imbalanced learning settings, fine-grained accuracy (many/medium/few group accuracy) is commonly reported in multi-class class-imbalanced learning settings.) Further, we repeated the experiments on the CIFAR datasets five times with various random seeds, and measured the average accuracy over repeated experiments. As in other CIL studies, we set a deep CNN as ResNet-32 [23].

ImageNet-LT [47] is a large-scale long-tailed dataset created from ImageNet-2012 [16], where the class distribution of 1000 classes follows a Pareto distribution with $N_1 = 1280$ and $N_{1000} = 5$. Each image was resized to 224×224 , and the images were augmented with random crop, horizontal flip, and color jitter. Following previous studies, we conducted experiments on ImageNet-LT by setting deep CNNs as ResNet-10, ResNet-50, and ResNeXt-50 [70].

iNaturalist2018 [62] is a large-scale dataset comprising real-world animals and plants, where 8142 classes follows an extremely imbalanced distribution with $N_1 = 1000$ and $N_{8142} = 2$. Each image was resized to 224×224 , and the images were augmented with random crop and horizontal flip. As in other CIL studies, we conducted experiments on iNaturalist2018 with ResNet-50.

We measured the prediction accuracy for every 10 epochs on test sets of CIFAR-10 and CIFAR-100, and for every 20 epochs on test sets of ImageNet-LT and iNaturalist2018. For all the datasets, we trained DAMEL for 200 epochs using the stochastic gradient descent (SGD) optimizer with a learning rate of 0.1 and a momentum of 0.9, similar to the Ace study [4]. The EMA update hyperparameter β was set to 0.1. We report the results of DAMEL with three and four experts for ImageNet-LT and iNaturalist2018. Further details regarding the hyperparameter settings and implementation are described in Appendix C. We compared the performance of DAMEL with the baseline algorithms compared in ACE [4] and RIDE [64]. Specifically, we considered **1. vanilla algorithm** - naive deep CNN trained using the cross-entropy loss. **2. CIL algorithms** - OLTR [47], Resampling [6], M2m [34], Mixup [76], LDAM [5], Logit adj [49], BALMS [55], cRT, LWS, τ -norm [31], PACO [13], TSC [45], ProCo [18], Meta-CALA [79], and CSA [57], and **3. multi-expert learning algorithms** - BBN [78], LFME [69], RIDE [64], ACE [4], TLC [44], ResLT [12], and MCE [65]. Further details of the baseline algorithms are provided in the Appendix D.

4.2. Experimental Results

The prediction accuracy of the baseline algorithms and DAMEL trained on CIFAR-100-LT with $\gamma = 100$ are summarized in Table 2. We can observe that even with one expert (without aggregating representations), the proposed algorithm achieved best overall performance. These results demonstrate the effectiveness of aggregating weights along the time axis. By aggregating the representations of multiple experts, DAMEL produced even higher performance and achieved state-of-the-art performance for all groups of the Many, Medium, and Few classes. We can also observe that the performance of DAMEL consistently improved as the number of experts increased. In Section 4.3, we verify that the superior performance of DAMEL is resulted from the reduction of the squared bias and variance owing to the aggregation along the two axes.

Table 2: Prediction accuracy of baseline algorithms and DAMEL. The results were copied from ACE [4] and RIDE [64]. “-” indicate that the corresponding results are not reported in the paper. Algorithms with * aggregate the predictions of four experts.

CIFAR-100-LT with $\gamma = 100$				
Algorithm	Overall	Many	Medium	Few
Vanilla	38.3	65.2	37.1	9.1
Resampling [6]	36.0	59.0	35.4	10.9
Mixup [76]	41.2	70.7	40.4	8.8
LDAM+DRW [5]	42.0	61.5	41.7	20.2
LDAM+M2m [34]	43.5	-	-	-
Logit Adj [49]	43.9	-	-	-
cRT [31]	43.3	64.0	44.8	18.1
BBN [78]	39.4	47.2	49.4	19.8
LFME [69]	43.8	-	-	-
RIDE* [64]	49.1	69.3	49.3	26.0
ACE* [4]	49.6	66.3	52.8	27.2
TLC* [44]	49.8	71.1	48.4	29.7
DAMEL (1 expert)	50.0	66.5	51.0	30.3
DAMEL (2 experts)	52.1	69.5	53.1	31.2
DAMEL (3 experts)	52.6	70.4	53.5	31.5
DAMEL (4 experts)	53.1	71.6	53.8	31.4

Moreover, to evaluate the performance of DAMEL under various settings,

we conducted experiments on both CIFAR-10-LT and CIFAR-100-LT while changing the ratio of the class imbalance γ from 50 to 100. In Table 3, we can observe that DAMEL with four experts achieved a higher performance than the baseline algorithms under every setting.

Table 3: Prediction accuracy of baseline algorithms and DAMEL

Algorithm	CIFAR-10-LT		CIFAR-100-LT	
	$\gamma=100$	$\gamma=50$	$\gamma=100$	$\gamma=50$
Vanilla	69.8	75.2	38.3	42.1
Mixup [76]	73.1	77.8	41.2	45.0
LDAM+DRW [5]	77.0	79.3	42.0	45.1
LDAM+M2m [34]	79.1	-	43.5	-
Logit Adj [49]	77.7	-	43.9	-
TSC [45]	79.7	82.9	43.8	47.4
ProCo [18]	84.8	87.5	51.8	56.4
Meta-CALA [79]	84.8	-	52.3	-
CSA [57]	82.5	86.0	46.6	51.9
BBN [78]	79.8	82.2	39.4	47.0
RIDE [64]	81.7	84.0	48.0	52.2
ACE [4]	81.2	84.3	49.4	50.7
TLC [44]	80.3	-	49.0	-
ResLT [12]	-	85.4	-	52.8
MCE [65]	84.5	87.3	50.1	56.0
DAMEL (3 experts)	84.7	86.5	52.6	56.9
DAMEL (4 experts)	85.0	87.9	53.1	57.8

DAMEL and baseline algorithms in Table 2 and Table 3 were trained with weak data augmentation techniques such as random crop and random horizontal flip. To evaluate the performance of DAMEL over recent algorithms that use strong data augmentation, we performed additional experiments and compared the results in Table 4. For comparison, we considered BALMS [55] and PACO [13], which use AutoAugment [11] and Cutout [17] as the strong data augmentation techniques. For fair comparison, we also used AutoAugment and Cutout when training DAMEL. In Section 4, we can observe that DAMEL achieved higher performance than BALMS and PACO. These results show that DAMEL can also be well combined with advanced data augmentation techniques. We describe AutoAugment and Cutout in more detail in Appendix E.

Table 4: Prediction accuracy of algorithms trained with AutoAugment and Cutout.

CIFAR-100-LT			
Algorithm	$\gamma=100$	$\gamma=50$	$\gamma=10$
BALMS [55]	50.8	54.2	63.0
PACO [13]	52.0	56.0	64.2
DAMEL (3 experts)	54.5	58.3	66.6

Furthermore, we evaluated the performance of DAMEL on the large-scale datasets, ImageNet-LT and iNaturalist2018. In Table 5, we can observe that DAMEL with four experts consistently outperformed the baseline algorithms. These results show that DAMEL performs effectively even on large-scale datasets.

Table 5: Prediction accuracy of baseline algorithms and DAMEL

Algorithm	ImageNet-LT			iNaturalist
	Res10	Res50	ResX50	Res50
Vanilla	20.9	41.6	44.4	66.1
OLTR [47]	34.1	-	46.3	63.9
LDAM+DRW [5]	36.0	-	-	68.0
τ -norm [31]	40.6	46.7	49.4	65.6
cRT [31]	41.8	47.3	49.5	65.2
LWS [31]	41.4	47.7	49.9	65.9
Logit Adj [49]	-	51.1	-	66.4
TSC [45]	-	52.4	-	69.7
ProCo [18]	-	57.3	58.0	73.5
Meta-CALA [79]	-	-	55.1	74.1
CSA [57]	-	49.7	-	-
BBN [78]	-	48.3	49.3	68.0
LFME [69]	38.8	-	-	-
RIDE [64]	45.9	54.9	56.4	72.2
ACE [4]	44.0	54.7	56.6	72.9
TLC [44]	-	54.6	-	-
ResLT [12]	43.8	52.9	-	70.5
MCE [65]	-	-	58.8	73.2
DAMEL (3 experts)	47.7	56.8	58.3	73.6
DAMEL (4 experts)	48.8	57.7	59.5	-

4.3. Detailed Analysis of DAMEL

Based on the finding that a neural network with different parameter initializations finds a different mode in the optimization process [38], we argue that multiple experts learn different representations even if each expert is trained with the same loss. To verify this, we compared the visualizations of dimension-reduced features, particularly principal components [10, 43, 58], derived from representations learned from multiple experts using EigenCAM [32, 51]. In Figure 2 (b) and Figure 2 (d), we can observe that the first and third experts learned representations corresponding to the screw part of the corkscrew. Using these representations, the first and third experts correctly classified the image in Figure 2 (a) as the corkscrew. By contrast, the second expert learned different representations corresponding to the handle of the corkscrew and incorrectly classified the image as a neck brace. Nevertheless, the auxiliary classifier made a correct prediction because proper representations were delivered by the first and third experts. As can be seen in this example, aggregating representations from multiple experts gives the auxiliary classifier a higher chance of receiving appropriate representations, even when some experts learn incorrect representations. In addition to reducing the variance of the predictions owing to the ensemble effect, DAMEL can reduce the squared bias of the predictions by utilizing appropriate representations. We present more examples of multiple experts learning different representations in Appendix F.

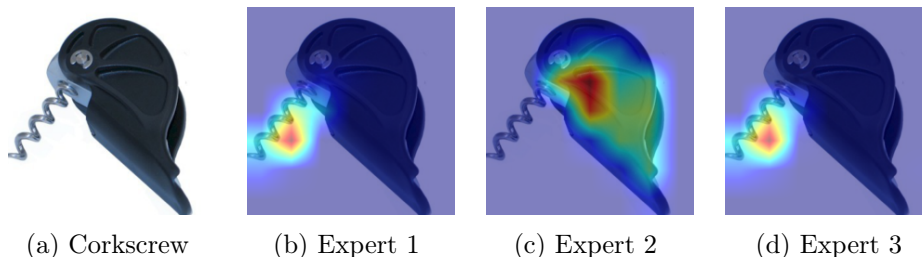


Figure 2: Image representations taken differently by multiple experts.

Moreover, we analyzed whether aggregating the representations of multiple experts results in better performance than aggregating predictions. In Table 6, we can observe that aggregating the representations of multiple experts consistently results in a higher performance. We can also observe that the performance gap between the two approaches increased as the number

of experts increased. This may be because the auxiliary classifier can use the information of the representations learned from multiple experts more effectively, as we analyzed in Figure 2. These results demonstrate that aggregating representations is more advantageous than aggregating predictions in making more accurate predictions using representations learned by all the experts.

Table 6: Prediction accuracy of DAMEL with aggregating predictions vs. representations of multiple experts on ImageNet-LT with ResNet-10.

Number of experts	Aggregation of predictions	Aggregation of representations
With 2 experts	45.8	46.6
With 3 experts	46.5	47.7
With 4 experts	46.9	48.3

We also argued that EMA weights stably approach the local optima in the space of test errors. To verify this, we measured test errors for algorithms trained with and without using EMA weights in Appendix A.

To verify our argument that using EMA weights can reduce the squared bias of predictions on minority classes, we also compared the confusion matrices of predictions on the test set of CIFAR-10-LT using the vanilla algorithm (trained with the cross-entropy loss), DAMEL without using EMA weights, RIDE, and DAMEL. The results are summarized in Appendix B.

Furthermore, to verify whether the use of the EMA weights and concatenated representations reduces both the squared bias and variance of the predictions, we quantitatively analyzed the squared bias and variance of the widely used baseline algorithms in Table 7. To measure the squared bias and variance of the predictions of multi-class classification algorithms, we replaced the predictions for the class of the highest predicted assignment probability with 1 and those for other classes with 0, following previous studies. We measured the squared bias and variance of predictions by repeating experiments for each algorithm 20 times while changing the random seed related to random sampling of a training set. In the case of the vanilla algorithm, the variance of the predictions was relatively low, but the squared bias of the predictions was significantly higher than that of the other algorithms, because the classifier was not trained with a class-balanced loss. Similar to the finding of [64], rebalancing techniques such as LDAM+DRW [5] and cRT

[31] reduced the squared bias of the predictions, but at the cost of increasing the variance compared to the vanilla algorithm. With multiple experts, RIDE [64] reduced the variance of the predictions and consequently improved the accuracy. We also measured the squared bias and variance of the predictions for "DAMEL without EMA weights" and "DAMEL without aggregating representations" to investigate the effect of the ensemble along each axis of DAMEL. We can observe that the ensemble along each axis reduces squared bias and variance of the predictions compared to the algorithms that do not use multiple experts. Using multiple experts along the dual axes, DAMEL further reduced both the squared bias and variance of the predictions.

Table 7: Analysis of the squared bias and variance of the predictions on CIFAR-100-LT with $\gamma=100$ using ResNet-32.

Algorithm	Bias ²	Variance	Accuracy
Vanilla (Cross entropy loss)	0.69	0.49	40.8
LDAM+DRW [5]	0.55	0.57	43.8
cRT [31]	0.59	0.52	44.3
RIDE [64]	0.59	0.43	48.9
DAMEL without using EMA weights	0.56	0.45	49.5
DAMEL without aggregating representations	0.54	0.46	50.0
DAMEL with 3 experts	0.53	0.42	52.6

4.4. Comparison with Iteration-Level EMA

To further analyze the proposed time-axis ensemble, we compare our epoch-level EMA with conventional iteration-level EMA. As shown in Table 8, epoch-level EMA consistently outperforms iteration-level EMA on both CIFAR-10-LT and CIFAR-100-LT under different imbalance ratios. This result indicates that the update frequency is important for constructing an effective time-axis ensemble.

Iteration-level EMA updates the averaged weights after every mini-batch, where consecutive model weights are highly correlated. Therefore, aggregating these highly similar weights may provide limited ensemble diversity. In contrast, epoch-level EMA updates the averaged weights only after the model has processed the entire training set, producing temporally more separated and diverse model states.

Table 8: Comparison between iteration-level EMA and epoch-level EMA.

EMA update frequency	CIFAR-10-LT		CIFAR-100-LT	
	$\gamma = 100$	$\gamma = 50$	$\gamma = 100$	$\gamma = 50$
Iteration-level EMA	81.7	84.4	48.5	53.2
Epoch-level EMA (Ours)	85.0	86.9	53.1	57.8

This is particularly useful in class-imbalanced learning, where mini-batch-level class compositions can be unstable under severe imbalance. Updating EMA at the epoch level reduces the influence of such mini-batch fluctuations and captures a more stable global training trajectory. As a result, DAMEL can obtain a more effective time-axis ensemble that reduces prediction variance while preserving later-stage learned representations.

4.5. Computational Cost Analysis

We analyze the computational cost of DAMEL by varying the number of experts as shown in Table 9. We report Floating point Operations per Second (FLOPs), GPU memory usage, the number of trainable parameters, and inference time on CIFAR-10-LT, CIFAR-100-LT, and ImageNet-LT. All measurements were conducted on an NVIDIA GeForce RTX 3090 Ti GPU.

Table 9: Computational cost analysis of DAMEL with different numbers of experts

Dataset	# Experts	FLOPs (iter/s)	GPU memory (MiB)	# Params	Inference time (s)
CIFAR-10-LT	1	46.5	1728	464,804	1.17
	2	40.4	1746	817,582	1.35
	3	35.5	1760	1,170,360	1.42
	4	32.0	1778	1,523,138	1.47
CIFAR-100-LT	1	44.7	1728	467,504	1.28
	2	38.2	1748	840,892	1.35
	3	34.2	1760	1,205,280	1.43
	4	30.1	1778	1,569,668	1.45
ImageNet-LT	3	2.67	15018	65,729,504	51.56
	4	2.54	15658	84,791,240	50.73

As the number of experts increases, the number of trainable parameters increases, while the FLOPs gradually decrease across all datasets. This trend

shows that DAMEL provides a practical performance-cost trade-off: increasing the number of experts can improve representation diversity and predictive performance, while requiring additional computational cost. Therefore, the number of experts can be selected according to the desired balance between accuracy and efficiency.

4.6. Capacity-controlled ablation study

To verify whether the gain of DAMEL comes from expert diversity rather than simply from increased representation dimensionality, we conducted a capacity-controlled ablation study. We constructed a single-expert model whose representation dimension matches the concatenated representation used in DAMEL. As shown in Table 10, this model consistently underperforms DAMEL on CIFAR-10-LT and CIFAR-100-LT, indicating that the improvement is not merely due to increased feature dimensionality or model capacity. Instead, the gain comes from combining diverse expert-specific representations. As shown in Figure 2 and Appendix Figure 5, different experts attend to different discriminative regions and learn complementary features, and representation concatenation allows the auxiliary balanced classifier to jointly exploit this complementary information.

Table 10: Capacity-controlled ablation study. The capacity-controlled model increases only the representation dimension without using multiple expert branches.

Method	CIFAR-10-LT		CIFAR-100-LT	
	$\gamma = 100$	$\gamma = 50$	$\gamma = 100$	$\gamma = 50$
Enlarged representation only	83.6	86.4	51.3	56.4
DAMEL (4 experts)	85.0	87.9	53.1	57.8

4.7. Sensitivity Analysis

To provide a more systematic analysis of DAMEL, we conduct sensitivity experiments on four key hyperparameters: the number of experts, the EMA update hyperparameter β , the classifier scale, and the class-balanced loss coefficient λ_{CB} . The results are summarized in Tables 11–14.

As shown in Table 11, increasing the number of experts generally improves the performance of DAMEL. This supports our argument that multiple experts provide more diverse representations, which can be effectively exploited by the auxiliary classifier.

Table 11: Sensitivity analysis on the number of experts.

# Experts	CIFAR-10-LT		CIFAR-100-LT		ImageNet-LT
	$\gamma = 100$	$\gamma = 50$	$\gamma = 100$	$\gamma = 50$	ResNet-50
1	81.8	84.9	50.0	53.8	-
2	82.1	85.5	52.1	56.3	-
3	84.7	86.5	52.6	56.9	56.8
4	85.0	87.9	53.1	57.8	57.7

As shown in Table 12, the EMA update hyperparameter β has a clear effect on performance. When β is too small, such as $\beta = 0.01$, the EMA weights are updated too slowly and do not sufficiently reflect recently learned network weights. In contrast, when β is too large, such as $\beta = 0.3$, the EMA weights overemphasize recent weights and lose the stabilizing benefit of temporal weight aggregation. The results suggest that moderate values, such as $\beta = 0.05$ or $\beta = 0.1$, provide a good balance.

Table 12: Sensitivity analysis on the EMA update hyperparameter β .

EMA β	CIFAR-10-LT		CIFAR-100-LT	
	$\gamma = 100$	$\gamma = 50$	$\gamma = 100$	$\gamma = 50$
0.01	81.1	83.3	49.0	54.5
0.05	84.8	86.9	52.4	57.0
0.10	84.7	86.5	52.6	56.9
0.20	84.1	86.4	51.4	56.0
0.30	83.3	85.6	50.1	55.0

Table 13 shows that DAMEL is not highly sensitive to the classifier scale within a reasonable range. In particular, scale values between 16 and 24 provide stable performance across datasets and imbalance ratios. This indicates that DAMEL does not rely on a highly specific classifier scale value.

Finally, Table 14 shows that the class-balanced loss coefficient λ_{CB} is also not highly sensitive within the tested range. DAMEL maintains stable performance across moderate variations of λ_{CB} , indicating that the method is robust to the strength of the auxiliary class-balanced loss.

Overall, these analyses show that DAMEL performs consistently across reasonable hyperparameter ranges while providing practical guidelines for

Table 13: Sensitivity analysis on the classifier scale.

Scale	CIFAR-10-LT		CIFAR-100-LT	
	$\gamma = 100$	$\gamma = 50$	$\gamma = 100$	$\gamma = 50$
8	84.4	86.8	50.7	54.2
16	84.4	86.5	52.6	56.4
20	84.7	86.5	52.6	56.9
24	84.2	86.2	52.1	56.7

Table 14: Sensitivity analysis on the class-balanced loss coefficient λ_{CB} .

λ_{CB}	CIFAR-10-LT		CIFAR-100-LT	
	$\gamma = 100$	$\gamma = 50$	$\gamma = 100$	$\gamma = 50$
0.5	84.3	86.9	52.3	56.7
1.0	84.7	86.5	52.6	56.9
1.5	84.4	87.2	52.5	56.7
2.0	84.3	86.8	52.1	56.7

selecting the number of experts, EMA β , classifier scale, and λ_{CB} .

4.8. Ablation Study

To investigate the effect of each element of DAMEL, we conducted a fine-grained ablation study on CIFAR-100-LT with $\gamma = 100$. The results are presented in Table 15. Results are summarized as follows. **1)** DAMEL with all elements achieved the highest accuracy. **2)** Without the EMA weights, prediction accuracy decreased. **3)** Without aggregating representations, prediction accuracy decreased. **4)** Without using a class-balanced loss for training the auxiliary classifier, the prediction accuracy significantly decreased. **5)** Averaging (rather than concatenating) the representations of multiple experts decreased prediction accuracy. **6)** By updating the EMA weights for each iteration (rather than each epoch). **7)** With simple averaging (SWA instead of EMA) of the network weights, prediction accuracy decreased. **8)** With a higher value or lower value of the EMA update hyperparameter ($\beta = 0.3$) and ($\beta = 0.01$), prediction accuracy decreased. Through repeated experiments with various β values, we found that β values between 0.05 and 0.2 updated the EMA weights appropriately. **9)** With decoupled learning of the

auxiliary classifier and representations of multiple experts, the prediction accuracy decreased. All these results verify that each element of DAMEL is useful.

Table 15: Ablation study for DAMEL on CIFAR-100-LT with $\gamma = 100$. Each row indicates the performance of DAMEL under the conditions described in that row.

Ablation study	Overall	Many	Medium	Few
DAMEL with 3 experts (proposed algorithm)	52.6	71.6	53.8	31.4
Without using EMA weights	39.5	54.7	37.9	22.6
Without aggregating representations (1 expert)	49.2	64.6	50.6	29.0
Without using class-balanced loss	46.4	75.3	46.4	13.4
With averaging the representations	50.0	66.8	50.1	28.2
With updating EMA weights for each iteration	48.5	62.4	50.3	28.8
With simple averaging of weights (SWA)	50.7	66.8	52.6	30.3
With higher EMA update hyperparameter ($\beta = 0.3$)	50.2	68.5	50.2	25.9
With lower EMA update hyperparameter ($\beta = 0.01$)	49.6	68.3	49.4	28.7
With decoupled learning of auxiliary classifier	46.7	67.4	44.5	25.5

To further verify the effectiveness of using the EMA weights in detail, we also conducted experiments on CIFAR-10-LT and CIFAR-100-LT with and without EMA weights while changing the number of experts in Appendix G.

5. Conclusion

We proposed DAMEL, a new CIL algorithm employing multiple experts along dual axes to mitigate both bias and variance of predictions. DAMEL encourages the auxiliary classifier to be trained with various representations by aggregating the representations of multiple experts. Additionally, DAMEL uses multiple experts along the time axis by updating the EMA weights at the end of each epoch. Experimental results across various scenarios demonstrate DAMEL’s superiority over other multi-expert learning and CIL algorithms. We conducted extensive qualitative analysis and ablation studies to validate each component of DAMEL. In this study, we set hyperparameters heuristically based on experimental results, lacking theoretical grounding. In future work, we aim to provide theoretical justification for determining the optimal number of multiple experts and the optimal EMA update hyperparameter.

Conflict of Interest Disclosure

The authors declare that they have no conflict of interests that could have appeared to influence the work reported in this manuscript.

References

- [1] An, J., Ying, L., Zhu, Y., 2021. Why resampling outperforms reweighting for correcting sampling bias with stochastic gradients, in: International Conference on Learning Representations.
- [2] Barandela, R., Rangel, E., Sánchez, J.S., Ferri, F.J., 2003. Restricted decontamination for the imbalanced training sample problem, in: Iberoamerican Congress on Pattern Recognition, Springer. pp. 424–431.
- [3] Blundell, C., Cornebise, J., Kavukcuoglu, K., Wierstra, D., 2015. Weight uncertainty in neural network, in: International Conference on Machine Learning, PMLR. pp. 1613–1622.
- [4] Cai, J., Wang, Y., Hwang, J.N., 2021. Ace: Ally complementary experts for solving long-tailed recognition in one-shot, in: Proceedings of the IEEE/CVF International Conference on Computer Vision, pp. 112–121.
- [5] Cao, K., Wei, C., Gaidon, A., Arechiga, N., Ma, T., 2019. Learning imbalanced datasets with label-distribution-aware margin loss, in: Wallach, H., Larochelle, H., Beygelzimer, A., d'Alché-Buc, F., Fox, E., Garnett, R. (Eds.), Advances in Neural Information Processing Systems, Curran Associates, Inc.
- [6] Chawla, N.V., Bowyer, K.W., Hall, L.O., Kegelmeyer, W.P., 2002. Smote: synthetic minority over-sampling technique. *Journal of Artificial Intelligence Research* 16, 321–357.
- [7] Cho, H., Koo, W., Kim, H., 2023. Prediction of highly imbalanced semiconductor chip-level defects in module tests using multimodal fusion and logit adjustment. *IEEE Transactions on Semiconductor Manufacturing* 36, 425–433.
- [8] Chou, H.P., Chang, S.C., Pan, J.Y., Wei, W., Juan, D.C., 2020. Remix: Rebalanced mixup, in: European Conference on Computer Vision, Springer. pp. 95–110.
- [9] Choy, M., Kim, D., Lee, J.G., Kim, H., Motoda, H., 2016. Looking back on the current day: interruptibility prediction using daily behavioral

- features, in: Proceedings of the 2016 ACM international joint conference on pervasive and ubiquitous computing, pp. 1004–1015.
- [10] Chung, J., Kim, H., 2019. Crime risk maps: A multivariate spatial analysis of crime data. *Geographical analysis* 51, 475–499.
 - [11] Cubuk, E.D., Zoph, B., Mane, D., Vasudevan, V., Le, Q.V., 2019. Autoaugment: Learning augmentation strategies from data, in: Proceedings of the IEEE/CVF Conference on Computer Vision and Pattern Recognition, pp. 113–123.
 - [12] Cui, J., Liu, S., Tian, Z., Zhong, Z., Jia, J., 2022. Reslt: Residual learning for long-tailed recognition. *IEEE Transactions on Pattern Analysis and Machine Intelligence* 45, 3695–3706.
 - [13] Cui, J., Zhong, Z., Liu, S., Yu, B., Jia, J., 2021. Parametric contrastive learning, in: Proceedings of the IEEE/CVF International Conference on Computer Vision, pp. 715–724.
 - [14] Cui, Y., Jia, M., Lin, T.Y., Song, Y., Belongie, S., 2019. Class-balanced loss based on effective number of samples, in: Proceedings of the IEEE/CVF Conference on Computer Vision and Pattern Recognition, pp. 9268–9277.
 - [15] Das, S., Mullick, S.S., Zelinka, I., 2022. On supervised class-imbalanced learning: An updated perspective and some key challenges. *IEEE Transactions on Artificial Intelligence* 3, 973–993.
 - [16] Deng, J., Dong, W., Socher, R., Li, L.J., Li, K., Fei-Fei, L., 2009. Imagenet: A large-scale hierarchical image database, in: 2009 IEEE conference on computer vision and pattern recognition, Ieee. pp. 248–255.
 - [17] DeVries, T., Taylor, G.W., 2017. Improved regularization of convolutional neural networks with cutout. *arXiv preprint arXiv:1708.04552* .
 - [18] Du, C., Wang, Y., Song, S., Huang, G., 2024. Probabilistic contrastive learning for long-tailed visual recognition. *IEEE Transactions on Pattern Analysis and Machine Intelligence* 46, 5890–5904.

- [19] Fan, Y., Dai, D., Kukleva, A., Schiele, B., 2022. Cossl: Co-learning of representation and classifier for imbalanced semi-supervised learning, in: Proceedings of the IEEE/CVF conference on computer vision and pattern recognition, pp. 14574–14584.
- [20] Fort, S., Hu, H., Lakshminarayanan, B., 2019. Deep ensembles: A loss landscape perspective. arXiv preprint arXiv:1912.02757 .
- [21] He, H., Garcia, E.A., 2009. Learning from imbalanced data. IEEE Transactions on knowledge and data engineering 21, 1263–1284.
- [22] He, K., Fan, H., Wu, Y., Xie, S., Girshick, R., 2020. Momentum contrast for unsupervised visual representation learning, in: Proceedings of the IEEE/CVF Conference on Computer Vision and Pattern Recognition, pp. 9729–9738.
- [23] He, K., Zhang, X., Ren, S., Sun, J., 2016. Deep residual learning for image recognition, in: Proceedings of the IEEE conference on computer vision and pattern recognition, pp. 770–778.
- [24] Howard, A., Sandler, M., Chu, G., Chen, L.C., Chen, B., Tan, M., Wang, W., Zhu, Y., Pang, R., Vasudevan, V., et al., 2019. Searching for mobilenetv3, in: Proceedings of the IEEE/CVF International Conference on Computer Vision, pp. 1314–1324.
- [25] Huang, C., Li, Y., Loy, C.C., Tang, X., 2016. Learning deep representation for imbalanced classification, in: Proceedings of the IEEE conference on computer vision and pattern recognition, pp. 5375–5384.
- [26] Iscen, A., Araujo, A., Gong, B., Schmid, C., 2021. Class-balanced distillation for long-tailed visual recognition. arXiv preprint arXiv:2104.05279 .
- [27] Izmailov, P., Podoprikin, D., Garipov, T., Vetrov, D., Wilson, A.G., 2018. Averaging weights leads to wider optima and better generalization, in: 34th Conference on Uncertainty in Artificial Intelligence 2018, UAI 2018, Association For Uncertainty in Artificial Intelligence (AUAI). pp. 876–885.
- [28] Jamal, M.A., Brown, M., Yang, M.H., Wang, L., Gong, B., 2020. Re-thinking class-balanced methods for long-tailed visual recognition from a

- domain adaptation perspective, in: Proceedings of the IEEE/CVF Conference on Computer Vision and Pattern Recognition, pp. 7610–7619.
- [29] JAPKOWICZ, N., 2000. The class imbalance problem: Significance and strategies, in: Proc. 2000 International Conference on Artificial Intelligence, pp. 111–117.
 - [30] Kang, B., Li, Y., Xie, S., Yuan, Z., Feng, J., 2020a. Exploring balanced feature spaces for representation learning, in: International Conference on Learning Representations.
 - [31] Kang, B., Xie, S., Rohrbach, M., Yan, Z., Gordo, A., Feng, J., Kalantidis, Y., 2020b. Decoupling representation and classifier for long-tailed recognition, in: International Conference on Learning Representations.
 - [32] Kho, S., Lee, P., Lee, W., Ki, M., Byun, H., 2022. Exploiting shape cues for weakly supervised semantic segmentation. *Pattern Recognition* 132, 108953.
 - [33] Kim, H., Kim, H., 2023. Contextual anomaly detection for high-dimensional data using dirichlet process variational autoencoder. *IJSE Transactions* 55, 433–444.
 - [34] Kim, J., Jeong, J., Shin, J., 2020. M2m: Imbalanced classification via major-to-minor translation, in: Proceedings of the IEEE/CVF Conference on Computer Vision and Pattern Recognition, pp. 13896–13905.
 - [35] Kim, K., Shin, J., Kim, H., 2021. Locally most powerful bayesian test for out-of-distribution detection using deep generative models. *Advances in Neural Information Processing Systems* 34, 14913–14924.
 - [36] Kong, H., Wang, L., 2023. Flexible model weighting for one-dependence estimators based on point-wise independence analysis. *Pattern Recognition* 139, 109473.
 - [37] Krizhevsky, A., 2009. Learning multiple layers of features from tiny images. Technical report, Department of Computer Science, University of Toronto .
 - [38] Lakshminarayanan, B., Pritzel, A., Blundell, C., 2017. Simple and scalable predictive uncertainty estimation using deep ensembles. *Advances in Neural Information Processing Systems* 30.

- [39] Lee, H., Lee, J., Kim, H., 2023a. Semi-supervised learning for simultaneous location detection and classification of mixed-type defect patterns in wafer bin maps. *IEEE Transactions on Semiconductor Manufacturing* 36, 220–230.
- [40] Lee, H., Park, T., Kim, H., 2025. Learnable logit adjustment for imbalanced semi-supervised learning under class distribution mismatch, in: *Proceedings of the IEEE/CVF International Conference on Computer Vision*, pp. 2664–2674.
- [41] Lee, H., Shin, S., Kim, H., 2021. Abc: Auxiliary balanced classifier for class-imbalanced semi-supervised learning. *Advances in Neural Information Processing Systems* 34.
- [42] Lee, H.H., Park, S., Im, J., 2023b. Resampling approach for one-class classification. *Pattern Recognition* , 109731.
- [43] Lee, K., Gray, A., Kim, H., 2013. Dependence maps, a dimensionality reduction with dependence distance for high-dimensional data. *Data Mining and Knowledge Discovery* 26, 512–532.
- [44] Li, B., Han, Z., Li, H., Fu, H., Zhang, C., 2022a. Trustworthy long-tailed classification, in: *Proceedings of the IEEE/CVF Conference on Computer Vision and Pattern Recognition*, pp. 6970–6979.
- [45] Li, T., Cao, P., Yuan, Y., Fan, L., Yang, Y., Feris, R.S., Indyk, P., Katabi, D., 2022b. Targeted supervised contrastive learning for long-tailed recognition, in: *Proceedings of the IEEE/CVF Conference on Computer Vision and Pattern Recognition*, pp. 6918–6928.
- [46] Li, T., Wang, L., Wu, G., 2021. Self supervision to distillation for long-tailed visual recognition, in: *Proceedings of the IEEE/CVF International Conference on Computer Vision*, pp. 630–639.
- [47] Liu, Z., Miao, Z., Zhan, X., Wang, J., Gong, B., Yu, S.X., 2019. Large-scale long-tailed recognition in an open world, in: *Proceedings of the IEEE/CVF Conference on Computer Vision and Pattern Recognition*, pp. 2537–2546.

- [48] Mehta, P., Bukov, M., Wang, C.H., Day, A.G., Richardson, C., Fisher, C.K., Schwab, D.J., 2019. A high-bias, low-variance introduction to machine learning for physicists. *Physics reports* 810, 1–124.
- [49] Menon, A.K., Jayasumana, S., Rawat, A.S., Jain, H., Veit, A., Kumar, S., 2020. Long-tail learning via logit adjustment, in: *International Conference on Learning Representations*.
- [50] Mikolov, T., Sutskever, I., Chen, K., Corrado, G.S., Dean, J., 2013. Distributed representations of words and phrases and their compositionality, in: Burges, C.J.C., Bottou, L., Welling, M., Ghahramani, Z., Weinberger, K.Q. (Eds.), *Advances in Neural Information Processing Systems*, Curran Associates, Inc.
- [51] Muhammad, M.B., Yeasin, M., 2020. Eigen-cam: Class activation map using principal components, in: *2020 International Joint Conference on Neural Networks (IJCNN)*, IEEE. pp. 1–7.
- [52] Nam, G., Yoon, J., Lee, Y., Lee, J., 2021. Diversity matters when learning from ensembles. *Advances in Neural Information Processing Systems* 34.
- [53] Park, S., Kim, K., Kim, H., 2022. Prediction of highly imbalanced semiconductor chip-level defects using uncertainty-based adaptive margin learning. *IISE Transactions* 55, 147–155.
- [54] Park, T., Lee, H., Kim, H., 2024. Rebalancing using estimated class distribution for imbalanced semi-supervised learning under class distribution mismatch, in: *European Conference on Computer Vision*, Springer. pp. 388–404.
- [55] Ren, J., Yu, C., sheng, s., Ma, X., Zhao, H., Yi, S., Li, h., 2020. Balanced meta-softmax for long-tailed visual recognition, in: Larochelle, H., Ranzato, M., Hadsell, R., Balcan, M.F., Lin, H. (Eds.), *Advances in Neural Information Processing Systems*, Curran Associates, Inc.. pp. 4175–4186.
- [56] Ren, M., Zeng, W., Yang, B., Urtasun, R., 2018. Learning to reweight examples for robust deep learning, in: *International Conference on Machine Learning*, PMLR. pp. 4334–4343.

- [57] Shi, J.X., Wei, T., Xiang, Y., Li, Y.F., 2023. How re-sampling helps for long-tail learning?, in: *Advances in Neural Information Processing Systems*.
- [58] Soh, W., Kim, H., Yum, B.J., 2018. Application of kernel principal component analysis to multi-characteristic parameter design problems. *Annals of Operations Research* 263, 69–91.
- [59] Tan, M., Chen, B., Pang, R., Vasudevan, V., Sandler, M., Howard, A., Le, Q.V., 2019. Mnasnet: Platform-aware neural architecture search for mobile, in: *Proceedings of the IEEE/CVF Conference on Computer Vision and Pattern Recognition*, pp. 2820–2828.
- [60] Tan, M., Le, Q., 2019. Efficientnet: Rethinking model scaling for convolutional neural networks, in: *International Conference on Machine Learning*, PMLR. pp. 6105–6114.
- [61] Tarvainen, A., Valpola, H., 2017. Mean teachers are better role models: Weight-averaged consistency targets improve semi-supervised deep learning results, in: *Proceedings of the 31st International Conference on Neural Information Processing Systems*, pp. 1195–1204.
- [62] Van Horn, G., Mac Aodha, O., Song, Y., Cui, Y., Sun, C., Shepard, A., Adam, H., Perona, P., Belongie, S., 2018. The inaturalist species classification and detection dataset, in: *Proceedings of the IEEE conference on computer vision and pattern recognition*, pp. 8769–8778.
- [63] Wang, P., Han, K., Wei, X.S., Zhang, L., Wang, L., 2021a. Contrastive learning based hybrid networks for long-tailed image classification, in: *Proceedings of the IEEE/CVF Conference on Computer Vision and Pattern Recognition*, pp. 943–952.
- [64] Wang, X., Lian, L., Miao, Z., Liu, Z., Yu, S., 2021b. Long-tailed recognition by routing diverse distribution-aware experts, in: *International Conference on Learning Representations*.
- [65] Wang, Y., Sun, K., Guo, C., Zhong, S., Liu, H., Ma, Y., 2024. Multiple contrastive experts for long-tailed image classification. *Expert Systems with Applications* 255, 124613.

- [66] Wang, Y.X., Ramanan, D., Hebert, M., 2017. Learning to model the tail, in: Guyon, I., Luxburg, U.V., Bengio, S., Wallach, H., Fergus, R., Vishwanathan, S., Garnett, R. (Eds.), *Advances in Neural Information Processing Systems*, Curran Associates, Inc.
- [67] Wei, H., Tao, L., Xie, R., Feng, L., An, B., 2022. Open-sampling: Exploring out-of-distribution data for re-balancing long-tailed datasets, in: *International Conference on Machine Learning*, PMLR. pp. 23615–23630.
- [68] Wen, Y., Vicol, P., Ba, J., Tran, D., Grosse, R., 2018. Flipout: Efficient pseudo-independent weight perturbations on mini-batches, in: *International Conference on Learning Representations*.
- [69] Xiang, L., Ding, G., Han, J., 2020. Learning from multiple experts: Self-paced knowledge distillation for long-tailed classification, in: *European Conference on Computer Vision*, Springer. pp. 247–263.
- [70] Xie, S., Girshick, R., Dollár, P., Tu, Z., He, K., 2017. Aggregated residual transformations for deep neural networks, in: *Proceedings of the IEEE Conference on Computer Vision and Pattern Recognition*, pp. 1492–1500.
- [71] Yin, X., Yu, X., Sohn, K., Liu, X., Chandraker, M., 2018. Feature transfer learning for deep face recognition with under-represented data. *arXiv e-prints* , arXiv–1803.
- [72] Yoon, H., Kim, H., 2026. Multimodal deep generative model for semi-supervised learning under class imbalance. *Technometrics* , 1–24.
- [73] Yoon, T., Kim, H., 2024. Uncertainty estimation by density aware evidential deep learning. *arXiv preprint arXiv:2409.08754* .
- [74] Zada, S., Benou, I., Irani, M., 2022. Pure noise to the rescue of insufficient data: Improving imbalanced classification by training on random noise images, in: *International Conference on Machine Learning*, PMLR. pp. 25817–25833.
- [75] Zhang, H., Cisse, M., Dauphin, Y.N., Lopez-Paz, D., 2017. mixup: Beyond empirical risk minimization. *arXiv preprint arXiv:1710.09412* .

- [76] Zhang, H., Cisse, M., Dauphin, Y.N., Lopez-Paz, D., 2018. mixup: Beyond empirical risk minimization, in: International Conference on Learning Representations. URL: <https://openreview.net/forum?id=r1Ddp1-Rb>.
- [77] Zhao, L., Shang, Z., Tan, J., Zhou, M., Zhang, M., Gu, D., Zhang, T., Tang, Y.Y., 2022. Siamese networks with an online reweighted example for imbalanced data learning. *Pattern Recognition* 132, 108947.
- [78] Zhou, B., Cui, Q., Wei, X.S., Chen, Z.M., 2020. Bbn: Bilateral-branch network with cumulative learning for long-tailed visual recognition, in: Proceedings of the IEEE/CVF Conference on Computer Vision and Pattern Recognition, pp. 9719–9728.
- [79] Zhou, X., Wu, O., Yang, N., 2025. Class and attribute-aware logit adjustment for generalized long-tail learning, in: Proceedings of the AAAI Conference on Artificial Intelligence.